Jr. of Industrial Pollution Control 34(1)(2018) pp 1811-1817
www.icontrolpollution.com
Research Article

A STUDY ON PRODUCTION OF OXIDANT BY DECOMPOSITION OF H_2O_2 ON MN BASED CATALYST AND NO OXIDATION

JUNG HEE JANG, WOO JIN SHIN AND GI BO HAN*

Plant Engineering Center, Institute for Advanced Engineering, 175-28, Goan-ro 51 Beon-gil, Baegam-myon,
Cheoin-gu, Yongin-si, Gyeonggi-do 449-863, Republic of Korea.

(Received 22 December, 2017; accepted 20 February, 2018)

Key words: H_2O_2, Catalytic conversion, NO oxidation, Dry oxidant

ABSTRACT

In this study, NO oxidation process was studied to increase the NO treatment efficiency of pollutant present in exhaust gas. H2O2 catalytic cracking was introduced as a method of producing dry oxidizing agents with strong oxidizing power. The K-Mn/Fe2O3 heterogeneous catalysts applicable to the H2O2 decomposition process were prepared and their physico-chemical properties were investigated. The prepared dry oxidant was applied to the NO oxidation process to treat the simulated exhaust gas containing NO, NO conversion rates close to 100% were confirmed at various flow rates (5, 10, 20 L/min) of the simulated flue gas.

INTRODUCTION

NO_x is a leading air pollutant produced during the combustion of fossil fuels such as coal and oil and discharged into the atmosphere (Qi and Yang, 2003). Many researchers have conducted studies designed to remove NO_x, and one of the most widely used techniques is selective catalytic reduction (SCR). However, the SCR process requires a high temperature to be efficient while using a catalyst, resulting in a prohibitive cost of installation and operation, lowering economic efficiency (Jang, *et al.*, 2015). The high temperature in the SCR is necessary for the difficult conversion of NO; therefore, a new process to oxidize NO to NO_2 is required. The present study investigates H_2O_2 catalyst decomposition as a means to produce a dry oxidant to use in NO to NO_2 conversion.

A number of recent studies have reported that a dry oxidant can be produced through the decomposition of H_2O_2 on a heterogeneous catalyst containing transition metals such as Fe and Zr as main components (Wang, *et al.*, 2016; Wang and Gui, 2013; Lin and Gurol, 1998; Hu, *et al.*, 2016; Lousada and Jonsson, 2010; Pham, *et al.*, 2009). In addition, literature shows that the H_2O_2 catalytic decomposition takes place at a relatively low temperature. If used in the oxidation process, high oxidation efficiency can be achieved at a low temperature (Wang, *et al.*, 2016; Wang and Gui, 2013; Lin and Gurol, 1998). Operating at low temperature and high efficiency is possible with simple equipment, and this process is likely to address the shortcomings of the SCR method of NO conversion processing (Adewuyi and Owusu, 2006; Ding, *et al.*, 2014). The present study involves both the NO oxidization process for treating NO in flue gas, which is difficult to convert, and the H_2O_2 catalyst decomposition process for production of dry oxidant for use in NO oxidation. Therefore, K-Mn/Fe_2O_3 was prepared and applied to the H_2O_2 catalyst decomposition process to investigate the effect of the catalyst's physicochemical characteristics on H_2O_2 catalyst decomposition. The prepared dry oxidant was also injected into the NO oxidization process at 5 L/min, 10 L/min, and 20 L/min flow rates of simulated flue gas to investigate NO treatment characteristics by the flow rate. The equation for the production of dry oxidant through H_2O_2 catalyst decomposition is shown in Eq. (1), and the NO oxidation equations for the dry oxidant are

---

***Corresponding authors email: gbhan@iae.re.kr**

shown from Eq. (2) to Eq. (5) (Mauldin, *et al.*, 2004; Thomas and Vanderschuren, 1997; Park, *et al.*, 2008).

MATERIAL AND METHODS

Preparation of K-Mn/Fe_2O_3 catalysts

(Fig. 1) shows the process of preparing Fe_2O_3-supported catalysts with a K-Mn-based active substance as a carrier. First, Fe_2O_3, a support, was prepared by stirring an appropriate amount of $Fe_2SO_4 \cdot 7H_2O$, a precursor, and dissolving it in distilled water, followed by a precipitation process which involved injecting a NH_4OH aqueous solution, a precipitator, until the pH value reached 9 or 10 (Jang and Han, 2016). The resulting precipitate was aged at room temperature for 4 hours and then dried overnight at 110°C to obtain a solid product, which was calcined at 700°C for 4 hours. The obtained Fe_2O_3 support was mixed with distilled water to create a slurry state. $MnC_{12}H_2O$, which is a precursor of the active substance, and an aqueous KOH solution, which is an additive precursor, were simultaneously introduced in an appropriate amount. The aqueous solution of NH_4OH was then added to the aqueous solution of the precursor and carrier to obtain a pH value of 9–10. The resulting precipitate was dried at 110°C overnight and then calcined at 700°C for about 4 hours to prepare a K-Mn/Fe_2O_3 catalyst.

Characterization of K-Mn/Fe_2O_3 catalysts

The effects of the physical and chemical properties of the prepared K-Mn/Fe_2O_3 catalysts on H_2O_2 decomposition were investigated using multiple techniques. The crystal structure and properties of the prepared K-Mn/Fe_2O_3 catalysts were investigated using X-ray powder diffraction (XRD) analysis. The qualitative and quantitative analysis of the surface of the sample and the chemical bonds of the constituent elements were investigated using X-ray photoelectron spectroscopy (XPS, K-Alpha model, Thermo Electron Corporation). The acid sites of K-Mn/Fe_2O_3, which was an additionally prepared heterogeneous catalyst, were investigated by conducting a temperature-programmed desorption (TPD) experiment using NH_3 gas. The experimental procedure included: adsorbing NH_3 gas at a concentration of about 10% vol. by pouring it through the fixed catalyst bed for 6 hours, increasing temperature from room temperature to 800°C while pouring N_2 gas at 5°C/min, and conducting acid characterization of desorbed NH_3 using a thermal conductivity detector (TCD). The characteristics of H_2O_2 catalyst decomposition were investigated by reacting 55 g of H_2O_2 and 0.1 g of the prepared catalyst on a scale, recording the weight change of the H_2O_2 every 2 seconds to compare and evaluate decomposition rates.

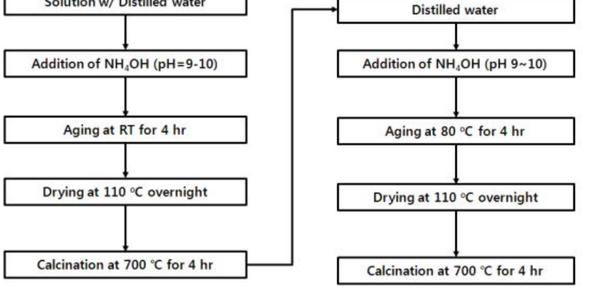

Fig. 1 Preparation of the catalyst for the catalytic H_2O_2 conversion.

Preparation of dry oxidant and NO oxidation using H_2O_2 catalytic decomposition

The production and oxidation of a dry oxidant using H_2O_2 catalyst decomposition for NO-containing flue gas treatments are shown in (Fig. 2). A metering pump capable of supplying H_2O_2 at about 500 ml/min and a vaporizer capable of converting it into a vapor state were installed. The evaporator installed in parallel for supplying H_2O_2 has a height of about 50 cm, a diameter of about 2 inches, and an inner volume of about 1 L. This ensures that the temperature can range from room temperature to about 400°C, and provides a structure which allows the H_2O_2 injected from the bottom by the metering pump to be discharged from the top after being converted into gas. Located at the back end were a stainless steel tubular reactor with a diameter of about 10 cm which could contain packed catalysts and a H_2O_2 decomposition reactor system capable of generating a dry oxidant. A chamber-type mixer was located such that the dry oxidant and the NO gas as the main target for reaction could be injected at the same time, and was connected to a stainless steel tubular oxidation reactor system of about 10 cm in diameter with a fixed bed of bead-type ceramic fillers installed. The H_2O_2 decomposition system, the oxidizing system, and the tube which the gases went through were equipped with an electric furnace and heating tapes, and the temperature at each section was controlled by installing a thermocouple (K-type) and then using an automatic temperature controller.

RESULTS AND DISCUSSION

Physicochemical characterization of K-Mn/Fe_2O_3

(Fig. 3) shows the results of XRD of the K-Mn/Fe_2O_3 and Fe_2O_3 catalysts. A Fe_2O_3 catalyst with rhombohedral structure crystallinity was

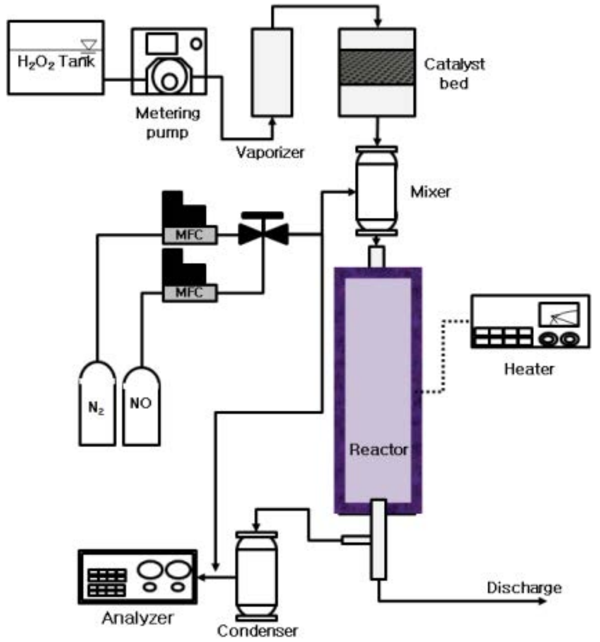

Fig. 2 Schematic diagram of the experimental setup for the catalytic H_2O_2 conversion and NO oxidation

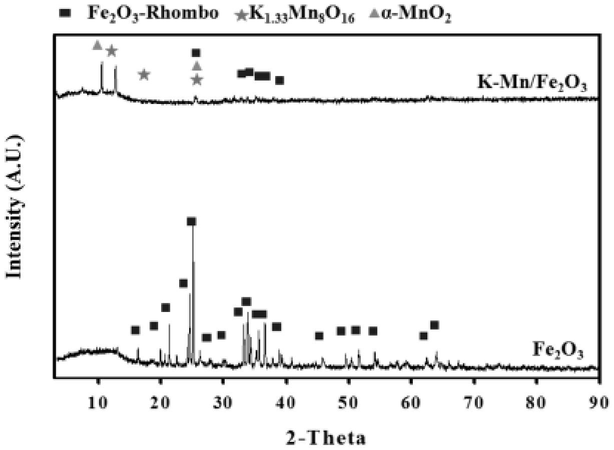

Fig. 3 XRD results of K-Mn/Fe_2O_3 and Fe_2O_3 catalysts.

obtained. The K-Mn/Fe_2O_3 catalyst prepared has a rhombohedral Fe_2O_3 structure as a support, and both the K1.33Mn8O16 compound form and the Fe_2O_3 compound form exist. (Fig. 4) shows the result of XPS analysis which involves measuring the binding energy of each element constituting the K-Mn/Fe_2O_3 catalyst, which carries K and Mn on Fe_2O_3 as a support. The results show that the peak of the Mn binding energy varied, but it appeared to be around the range that corresponds to 642.2 eV, and the form of the compound containing Mn that corresponds to the $KMnO_4$ binding range. As supporting evidence, measurements of the binding energy of K show that the peak was at 292.6 eV, suggesting that K also shows the binding structure of a $KMnO_4$-type compound. Measurements of the binding energy of Fe show the peak was at 710.1 eV, and the binding energy was that of Fe contained in a Fe_2O_3 compound. This suggests that the K-Mn/Fe_2O_3 catalyst is mostly composed of Fe_2O_3 supported by $KMnO_4$.

(Fig. 5a) shows the results of the NH_3-TPD experiment conducted to investigate the acidic properties of the prepared K-Mn/Fe_2O_3 catalyst. The NH_3 gas desorbed by adsorbing on the K-Mn/Fe_2O_3 catalyst, raising the temperature from room temperature to about 800°C at a rate of 5°C/min, and the amount of desorbed NH_3 was measured using a TCD. (Fig. 5) shows these measurements, including the temperature corresponding to each unit of NH_3 adsorption strength, and the adsorption amount of NH_3 gas corresponding to each unit of TCD detection strength. These results suggest that the amount of acid sites corresponding to the total amount of NH_3 adsorption can be determined as an integrated value for a linear graph corresponding to the amount of desorbed NH_3 as it varies by temperature. The total amount of acid sites for the NH_3 adsorption was found to be greater for K-Mn/Fe_2O_3 than for Fe_2O_3.

The total amount of acid sites, and the strengths and distribution of acid sites are shown in (Fig. 5b). The K-Mn/Fe_2O_3 catalyst, which has a relatively high amount of acid sites, shows a relatively even distribution of acid sites varying in strength, approximately corresponding to 217, 297, 355, 399, 452, 689, and 762°C. The amount of acid sites varied between 0.066 and 1.337 mmol/g.

Efficiency of H_2O_2 decomposition on the K-Mn/Fe_2O_3 catalyst

(Fig. 6a) shows conversion efficiency as H_2O_2 decomposition efficiency with a K-Mn/Fe_2O_3 catalyst for the production of dry oxidant. The amount of H_2O_2 injected for decomposition was about 0.3 g/min, the amount of catalyst was 1 g, and the flow rate was about 300 ml/min. The catalysts used in the experiment were K-Mn/Fe_2O_3 and Fe_2O_3, and the decomposition temperature of H_2O_2 was 150°C. The catalyst with the highest H_2O_2 decomposition efficiency was K-Mn/Fe_2O_3. This result likely hinges on the acid site distribution of the catalysts corresponding to the adsorption point, which is the physicochemical property of catalysts that are strongly associated with H_2O_2 decomposition characteristics. This is because the status and reactivity of H_2O_2 decomposition reactions depends on the electron mobility in the oxidation-reduction reaction, and this characteristic is related to the Lewis acid point of solid catalysts. In addition, the size of the reactivity likely depends on the distribution and

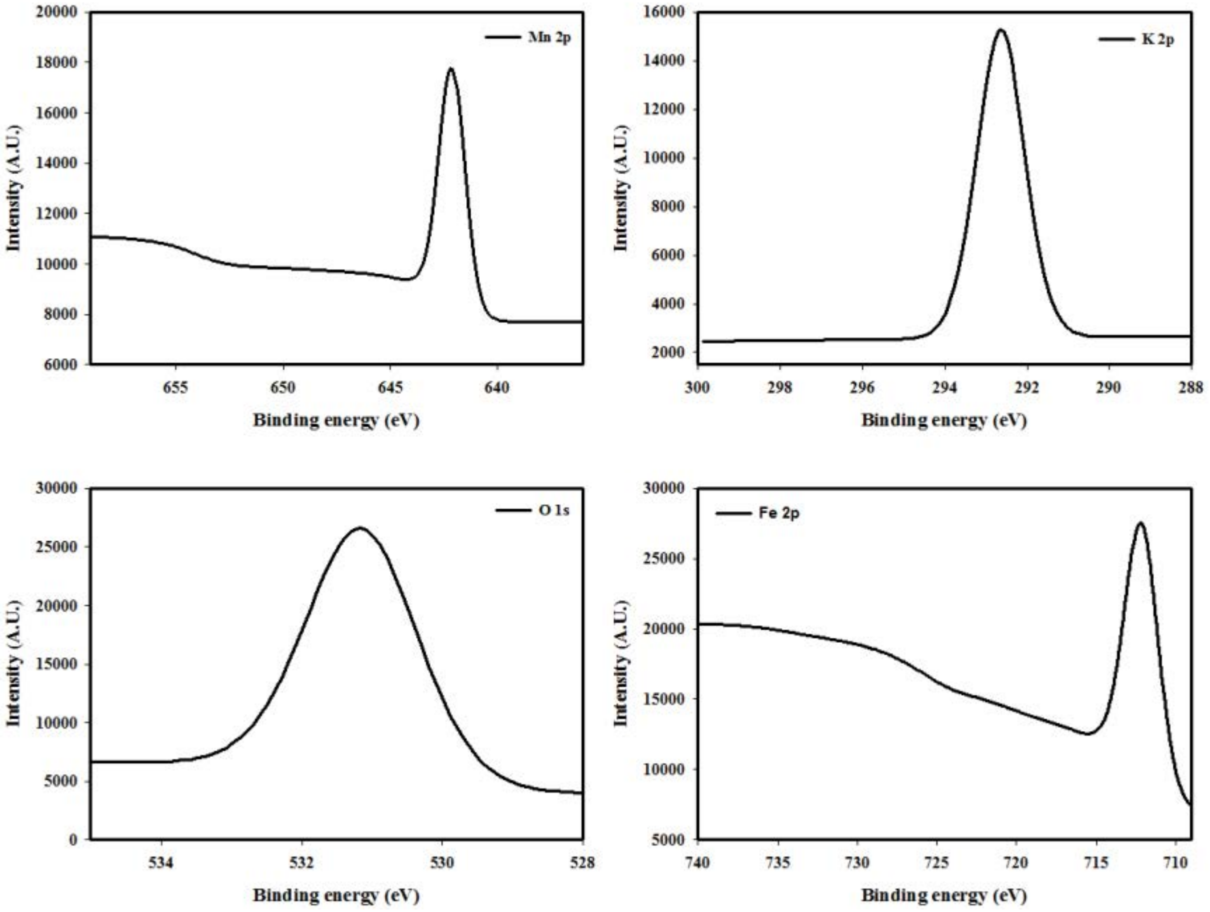

Fig. 4 XPS results of K-Mn/Fe_2O_3 catalysts.

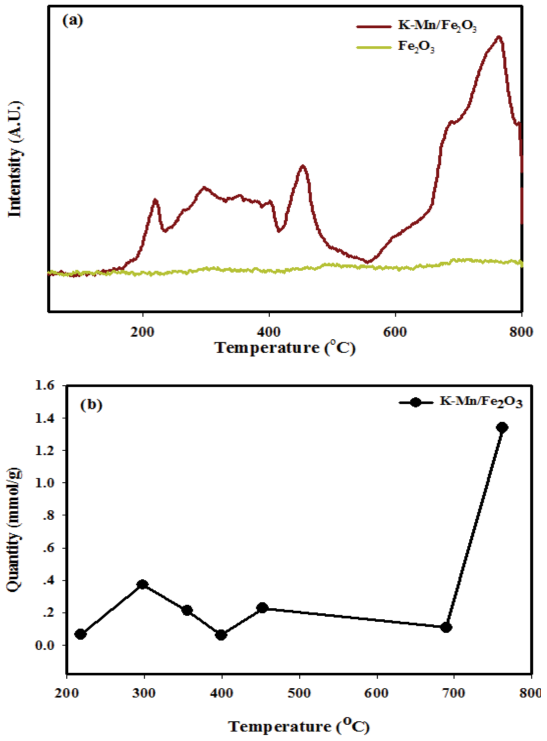

Fig. 5 NH_3-TPD results of K-Mn/Fe_2O_3 catalysts.

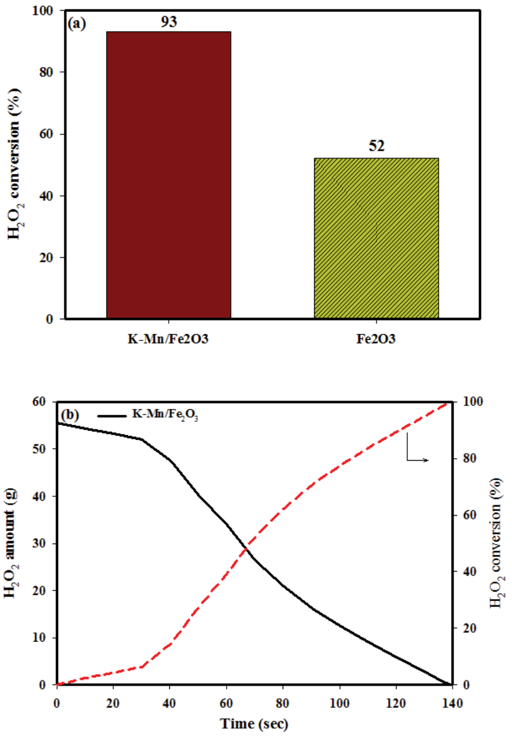

Fig. 6 Effect of the oxidation temperature on the NO oxidation.

amount of weak acid sites H_2O_2 has. (Fig. 6b) shows the amount of H_2O_2 decomposition by catalyst in the experiment. The results show that the decomposition efficiency of H_2O_2 gradually increases over time, and the time taken until the decomposition efficiency of the H_2O_2 catalyst (i.e., reaction rate) is stabilized by the K-Mn/Fe_2O_3 catalyst is 140 seconds.

Oxidation process of NO with dry oxidant obtained from H_2O_2 decomposition by treatment scale

(Fig. 7) shows the results on NO conversion efficiency, which were obtained by simultaneously injecting the dry oxidant obtained from the H_2O_2 decomposition reaction into the NO oxidation process along with the simulated flue gas. In the decomposition process, the reaction temperature was maintained at 150°C, and the H_2O_2 injection amount and the amount of catalyst fillers were 0.3 g/min and 0.5 g, respectively. In the oxidation process, the reaction temperature was varied from 40 to 150°C, and the flow rate of the injected simulated flue gas and the NO concentration in the gas were 300 ml/min and 1,000 ppm, respectively. The NO conversion efficiency depended on the reaction temperature of the oxidation process. As the NO conversion efficiency increased with reaction temperature, the NO conversion efficiency reached about 100% at about 150°C.

Fig. 8a) shows how the H_2O_2 injection amount affected the efficiency of the oxidation process. This was done by varying the injection amount of H_2O_2 by diluting it with distilled water to a 28% concentration, which is commonly used in the H_2O_2 decomposition process for dry oxidant production/supply, while maintaining the concentration and the flow rate of simulated flue gas injected into the oxidation process at about 1,000 ppm and 5 L/min. The reaction temperature in the H_2O_2 catalytic decomposition reactor system was about 150°C. Using the dry oxidant generated in the H_2O_2 decomposition process in the NO oxidation process, the reaction temperature was maintained at about 150°C. This was done to determine the conversion efficiency of NO, the treatment target gas, and the selectivity of NO_2, which is often generated in the oxidation reaction, according to the amount of H_2O_2 injected. As shown in (Fig. 8a), as the H_2O_2 injection amount increases from 1.6 to 20 ml/min, the concentration of NO as the primary conversion target gradually decreased and the concentration of NO_2 as the primary product gradually increased. There is a clear trend that NO conversion efficiency, along with NO_2, selectivity increases with the amount of H_2O_2 injected. This trend likely results from the increase in the amount of dry oxidant generated by the H_2O_2 reactor system as H_2O_2 injection amount increases, increasing the efficiency of NO oxidation.

(Fig. 8b) shows how the H_2O_2 injection amount affected the efficiency of the oxidation process as in (Fig. 8a) but at 10L/min. Compared to the 5 L/min

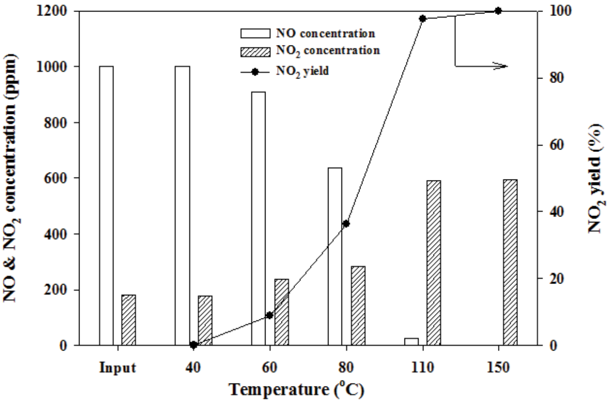

Fig. 7 Effect of the oxidation temperature on the NO oxidation.

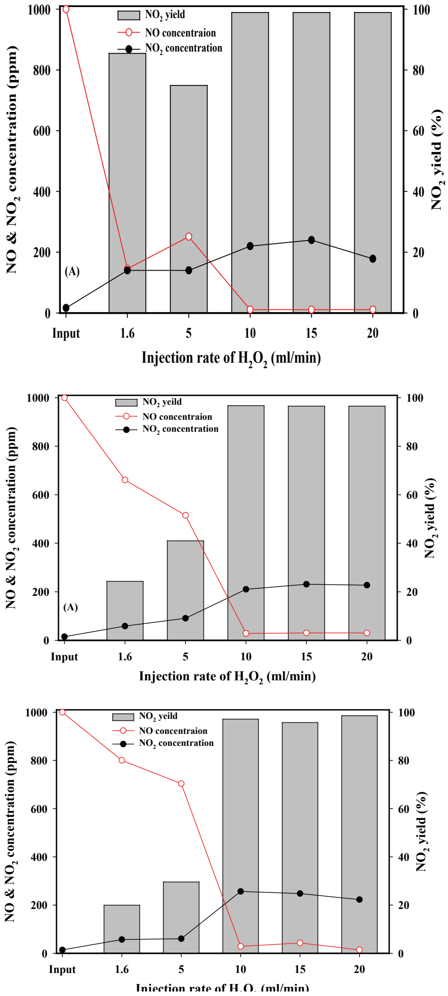

Fig. 8 Effect of the gas flow rate on the NO oxidation (Flow rate: a: 5, b: 10, c: 20 L/min).

flow rate condition, the experiment with the 10 L/min flow rate showed that conversion efficiency was sensitive to changes in the amount of H_2O_2 as the treatment capacity of the simulated flue gas supplied to the oxidation process increased. The increase in the NO_2 conversion efficiency also became larger as the injection amount of the H_2O_2 injection was increased in the flow rate range up to 10 ml/min.

As with (Fig. 8a and 8b), shows how the H_2O_2 injection amount affected the efficiency of the oxidation process at 20 L/min. Compared to the 5-10 L/min flow rate conditions, the experiment with the 20 L/min flow rate showed that conversion efficiency was sensitive to changes in the amount of H_2O_2 as the treatment capacity of the simulated flue gas supplied to the oxidation process increased. However, the increase rate in conversion compared to the increase in treatment capacity from 10 to 20 L/min was somewhat lower than that for the increase from 5 to 10 L/min. Therefore, it is advised that future studies incorporate this finding in the development of the scale-up process of the H_2O_2 catalyst decomposition combined with oxidization process.

CONCLUSION

The present study investigated NO conversion efficiency by generating dry oxidant through H_2O_2 decomposition on a K-Mn/Fe_2O_3 heterogeneous catalyst and injecting it into the NO oxidation process. The results of the physicochemical analysis and the decomposition of Mn-based K-Mn/Fe_2O_3 catalyst, in which Fe_2O_3 was used as a support and K was added, showed that the property of acidity has the greatest effect on the decomposition efficiency of H_2O_2. In addition, when the dry oxidant produced through H_2O_2 catalyst decomposition was injected into the NO oxidation process, the conversion efficiency reached close to 100%. Conversion efficiency increased with reaction temperature. In the NO oxidation process with varying flue gas flow rates, the NO conversion efficiency increased, reaching nearly 100%, as the H_2O_2 injection amount increased. These results are expected to inform the design of scale-up integrative process systems in the development of combined H_2O_2 catalyst decomposition and NO oxidation processes in the future.

ACKNOWLEDGEMENT

This study was supported by the Ministry of Environment's environmental industry advancement technology development project.

REFERENCES

Adewuyi, Y.G. and Owusu, S.O. (2006). Ultrasound-induced aqueous removal of nitric oxide from flue gases: Effects of sulfur dioxide, chloride, and chemical oxidant. *J. Phys. Chem. A*. 110 : 11098-11107.

Ding, J., Zhong, Q., Zhang, S., Song, F. and Bu, Y. (2014). Simultaneous removal of NOX and SO2 from coal-fired flue gas by catalytic oxidation-removal process with H_2O_2. *Chem. Eng. J.* 243 : 176-182.

Hu, H., Zha, K., Li, H., Shi, L. and Zhang, D. (2016). In situ DRIFTs investigation of the reaction mechanism over MnOx-MOy/$Ce_{0.75}$ $Zr_{0.25}O_2$ (M = Fe, Co, Ni, Cu) for the selective catalytic reduction of NOx with NH3. *Applied Surface Science*. 387 : 921-928.

Jang, H,H. and Han, G,B. (2016). A study on the NO oxidation using dry oxidant produced by the catalytic conversion of H_2O_2. *J. of Korean Oil Chemists' Soc.* 33 : 100-109.

Jang, J. H., Choi, H.Y. and Han, G.B. (2015). Production of dry oxidant through catalytic H_2O_2 decomposition over Mn-based catalysts for NO oxidation. *Clean Technology*. 21 : 130-139.

Lin, S.S. and Gurol, M.D. (1998). Catalytic decomposition of hydrogen peroxide on iron oxide: Kinetics mechanism and implications. *Environ. Sci. Technol.* 32 : 1417-1423.

Lousada, C.M. and Jonsson, M. (2010). Kinetics mechanism and activation energy of H_2O_2 decomposition on the surface of ZrO_2. *J. Phys. Chem. C*. 114 : 11202-11208.

Mauldin, R.L., Kosciucha, E., Henrya, B., Eiselea, F.L. and Shettera, R. (2004). Measurements of OH, HO_2 + RO_2, H_2SO_4, and MSA at the south pole during ISCA 2000. *Atmos. Environ.* 38 : 5423-5437.

Park, S.Y., Deshwal, B.R. and Moon, S.H. (2008). NOX removal from the flue gas of oil-fired boiler using a multistage plasma-catalyst hybrid system. *Fuel Process. Technol.* 89 : 540–548.

Pham, A.L.T., Lee, C., Doyle, F.M. and Sedlak, D.L.A. (2009). Silica-supported iron oxide catalyst capable of activating hydrogen peroxide at neutral pH values. Environ. Sci. Technol. 43 : 8930-8935.

Qi, R. and Yang, R.T. (2003). Low-temperature selective catalytic reduction of NO with NH_3 over iron and manganese oxides supported on Titania. *Appl. Catal. B*. 44 : 217-225.

Thomas, D. and Vanderschuren, J. (1997). Modeling of NOX absorption into nitric acid solutions containing hydrogen peroxide. *Ind. Eng. Chem. Res.* 36 : 3315–3322.

Wang, X. and Gui, K. (2013). Fe_2O_3 particles as superior catalysts for low temperature selective catalytic reduction of NO with NH_3. *Journal of Environmental Sciences*. 25 : 2469-2475.

Wang, X., Wu, S., Zou, W., Yu S., Gui K. and Dong L. (2016). Fe-Mn/Al_2O_3 catalysts for low temperature selective catalytic reduction of NO with NH_3. *Chinese Journal of Catalysis*. 37 : 1314-1323.